ELSEVIER

Journal of Nuclear Materials 241–243 (1997) 1087–1092

journal of nuclear materials

Deuterium trapping in and release from tungsten carbide

Wenmin Wang [a,b,*], V.Kh. Alimov [a,c], B.M.U. Scherzer [a], J. Roth [a]

[a] *Max-Plank-Institut für Plasmaphysik, EURATOM-Association, D-85748 Garching, Germany*
[b] *Shanghai Institute of Nuclear Research, Academia Sinica, P.O. Box 800-204, Shanghai 201800, China*
[c] *Institute of Physical Chemistry of the Russian Academy of Sciences, Moscow, Russia*

Abstract

Tungsten carbide coating, $W_{60}C_{40}$ and $W_{85}C_{15}$ prepared by chemical vapor deposition and consisting of different carbide phases, are implanted with 0.8, 1.5 and 3 keV deuterium ions at room temperature and elevated temperatures. The trapping and release of deuterium are investigated by means of re-emission and thermal desorption spectroscopy. The results have been compared with previous data from graphite and from tungsten prepared by various methods. It is found that a few percent of carbon impurities strongly increases the deuterium inventory in tungsten. The thermal desorption of deuterium from tungsten carbide occurs at temperatures much lower than for graphite and the spectral form shows much more complicated features. The peak temperatures, in this case, mainly depends on the carbon concentration in different phases of the samples. Chemical erosion is only detected for sample $W_{60}C_{40}$. In this case all carbon atoms are eroded as volatile hydrocarbons while the physical sputtering of tungsten atoms limits the total erosion. Both fluence and temperature dependence of the chemical erosion are very similar to the results from the interaction of TiC with keV hydrogen ions.

Keywords: Wall particle retention; High Z wall material

1. Introduction

The high Z material tungsten has been proposed as a plasma-facing material for the future fusion experiment ITER. In order to get the data base for ITER, tungsten-coated graphite tiles have been installed as divertor target in the tokamak ASDEX Upgrade for the campaign starting at the end of 1995. Based on previous calculation and experiments, a tungsten carbide layer could be formed during the bombardment of tungsten by carbon impurity ions [1]. Besides erosion of tungsten, the analysis of tungsten tiles from ASDEX Upgrade also shows a pronounced deposition of carbon, originating from the vessel walls, on the tungsten probe. Deposited layers with thickness of a few hundred nm to over 20 μm have been found in a wide range of carbon atomic ratio between 5% to 40% at the different locations of the tungsten probe [2]. In view of the above mentioned fact, not only pure materials, such as carbon and tungsten, should be studied, but also the tungsten carbide and carbon-containing tungsten.

Hydrogen trapping in and thermal release from wall materials during plasma–surface interaction are important factors determining tritium inventory in the first wall and divertor in the future fusion machine. Over the last decade, the re-emission and thermal desorption of hydrogen from carbon and some carbon based materials have been thoroughly investigated. However, there is only little work done on the interaction with tungsten [3–6] and no data on tungsten carbide is reported. In this work the re-emission of deuterium in different molecular forms of D_2, HD and CD_4 from tungsten carbide during deuterium bombardment is studied as well as the deuterium retention and thermal desorption. The behaviour that is different from graphite and tungsten is discussed.

2. Experimental

Tungsten carbide layers were chemically deposited on the substrates of copper or tungsten from a vapor mixture

* Corresponding author. Fax: +49-89 3299 1149.

PII S0022-3115(96)00665-4

of tungsten fluorides, carbon-containing gases and hydrogen at the temperature of 750–900 K. The grain size of the coating is about 1 μm and the surface roughness is 1–2 μm. The details of the target preparation are described in Refs. [7,8]. Two tungsten carbide targets, which were prepared in Moscow, were investigated in this work. The first is a tungsten carbide layer with an atomic ratio of W:C = 6:4. This CVD coating is about 11 μm on the substrate of tungsten, consisting of W_2C and $W_{12}C$ carbide phases together with 10–20 at% carbon atoms. The second is a tungsten carbide layer with an atomic ratio of W:C = 85:15. The coating, consisting of W_2C and $W_{12}C$ phases with some free tungsten atoms, is deposited on the substrate of copper with a thickness of 10–15 μm [7,8]. The atomic ratios of both targets were determined by XPS (X-ray photoelectron spectroscopy) after the surface was sputter-cleaned by 3 keV Ar^+ with a fluence of about $4.2 \times 10^{16}/cm^2$ to remove impurities on the surfaces. The impurity consisted essentially in a superficial layer containing less than 10 at% oxygen and nitrogen with a thickness of about two monolayers as inferred from the sputter cleaning time. On the $W_{60}C_{40}$ coating, a carbon rich layer of about 20 nm had to be removed before reaching the constant bulk concentration. The grain size and layer thickness of the tungsten carbide coatings were confirmed by scanning electron spectroscopy.

The re-emission and TDS (thermal desorption spectroscopy) were performed in the implantation chamber BOMBARDINO that has been described elsewhere [9,10]. The targets were mounted on a movable holder in a closed box to which a quadrupole mass spectrometer (QMS) is connected. The targets can be heated up to 1200 K by a resistive-heater fixed to the target holder. The temperature of the target surface is measured by a thermocouple attached directly to the target surface. Liquid nitrogen flows through a cold trap during the experiment in order to reduce the residual partial pressure of H_2O to a negligible value. The samples, which were pre-heated at 1200 K for a few minutes to release adsorbed gas from the target surface, were bombarded by normal incidence of D_3^+ with energies of 2.4, 4.5 and 9 keV at temperatures from 300 to 1020 K. The ion beam is swept both horizontally and vertically over a diaphragm of 1.5 mm diameter in front of the target in order to establish a homogeneous current distribution. The flux densities are kept at 1.5×10^{14}, 6.4×10^{14} and 1.7×10^{15} $D^+/(cm^2\ s)$ for the D^+ implantation energy of 0.8, 1.5 and 3 keV, respectively. The partial currents of re-emitted deuterium in the molecular forms of D_2 (mass 4), HD (mass 3) and CD_4 (mass 20) are recorded by the QMS. The QMS starts recording the residual partial pressure signals at 30–50 s before switching on the ion beam to get the background information. The signals were calibrated against the incident ion current when steady state re-emission (i.e. 100% re-emission) conditions were reached. For calibration of the CD_4 pure graphite was bombarded under conditions with well known CD_4 re-emission yield i.e. with 1.5 keV D^+ at 850 K for comparison [11]. Taking account of the number of D atoms per molecule, the re-emission rate of deuterium, n_D^{reem}, can be expressed by the following [12]:

$$n_D^{reem} = k\left[\alpha I_{HD} + 2\beta I_{D_2} + 4\gamma I_{CD_4}\right]. \quad (1)$$

I_{HD}, I_{D2} and I_{CD4} are the partial currents of QMS for mass 3 (HD), mass 4 (D_2) and mass 20 (CD_4). α, β and, γ are the normalizing factors for HD, D_2 and CD_4. Scaling the factor to unity for D_2 i.e. $\beta = 1$, we take $\alpha = 0.69$ from a normalization including the ionization probability, the cracking pattern in the ionizer and the transmission of the molecules through the quadrupole to the detector [11]. The QMS signal of CD_4 is calibrated by the experiments of re-emission of D from a graphite target bombarded with 1.5 keV D^+ at the temperature of 850 K in the same chamber of BOMBARDINO. Taking the value $Y = 0.065$ CD_4/D^+ for graphite [11] (the CD_4 yield of graphite bombarded under the same conditions, which was carefully investigated in a high current ion source at Garching), we get the factor $\gamma = 0.54$. Putting these factors into Eq. (1), we can quantitatively calculate the re-emission rate of deuterium. The factor k is determined from experiments at a high implantation fluence when the partial currents keep stationary values and re-emission is 100%. In this case the re-emission rate, n_D^{reem}, equals the implantation flux.

TDS was carried out after implantation at 300 K. The targets were heated up to 1200 K at a heating rate of 4.5 ± 0.7 K/s. The partial currents of the desorbed particles, D_2, HD and CD_4, were detected by QMS. Using the factor k determined from the re-emission measurements, we can quantitatively calculate the thermal desorbed deuterium.

3. Results and discussion

3.1. Deuterium re-emission

Fig. 1 shows the deuterium re-emission in different molecular forms (HD, D_2 and CD_4) from the target $W_{60}C_{40}$ bombarded with 1.5 keV D^+ at room temperature. The D_2 and HD signals are observed immediately after switching on the D^+ beam. The HD release reaches a steady value of 12% already at fluence of 1×10^{17} D^+/cm^2, while the D_2 signal increases steeply up to 18%, corresponding to a steep increase up to 30% for total deuterium re-emission. This fluence dependence can be attributed to the initial reflection of D atoms recombing at the inner walls of the closed box with adsorbed hydrogen and deuterium atoms. Then the D_2 signal increases gradually to 80% at a fluence of 3.2×10^{18} D^+/cm^2. In contrast, the release of CD_4 appears only after an initial deuterium accumulation in the implanted surface. The contribution of CD_4 increases

quickly and reaches a maximum of 18% at a fluence of about 3.5×10^{17} D^+/cm^2. Then it decreases steadily to a value of 0.08, equivalent to a methane formation yield of 0.02 CD_4/D^+, at the fluence of 3.2×10^{18} D^+/cm^2. Because of the current limit in the device of BOMBARDINO, the partial releases of D_2 and CD_4 do not reach their stable values after a bombardment for 1.5 h. An additional experiment was performed until 1.1×10^{19} D^+/cm^2 at a high current ion source. The release of CD_4 decreases to 0.01 CD_4/D^+ finally. At elevated temperatures the 100% re-emission levels are achieved at low fluences between $(0.4–5) \times 10^{17}$ D^+/cm^2. No initial high methane release is observed and the steady value of methane release shows a weak temperature dependence that will be discussed later in Fig. 2.

The surprising result is the high initial methane emission at room temperature. The maximum is a factor of 4.5 higher than the steady value, 0.01 CD_4/D^+. A very similar fluence dependence was previously found in the interaction of TiC with energetic hydrogen ions by Yamada et al. [13]. Their results suggested that the level of initial high methane release is dominated by the pre-bombardment history of the target. However, this can not explain our results. In the present case, if the target was annealed at high temperature between two implantation runs, the high initial methane release is always observed on a previously bombarded spot of the target (no matter how many times it was bombarded) and is very similar to the methane release from a new point at the target. The high initial methane release and a subsequent long decrease with fluence may be interpreted as surface segregation of carbon induced by ion bombardment, leading to a depletion throughout the ion range. This assumption has been checked by a preliminary Auger experiment during a bombardment with 1.5 keV D^+ at room temperature [14]. The AES measurement shows a pronounced high surface concentration of carbon and a sequential strong decrease until even a pure tungsten surface layer remains. The high initial release of methane

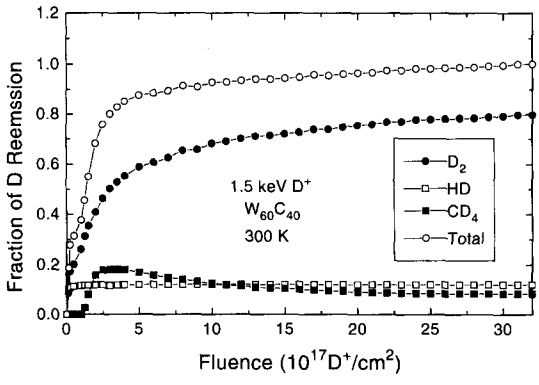

Fig. 1. Fractions of deuterium re-emission in the forms of D_2, HD and CD_4 from $W_{60}C_{40}$ during D^+ bombardment with a flux of 6.4×10^{14} $D^+/(cm^2\ s)$ at room temperature.

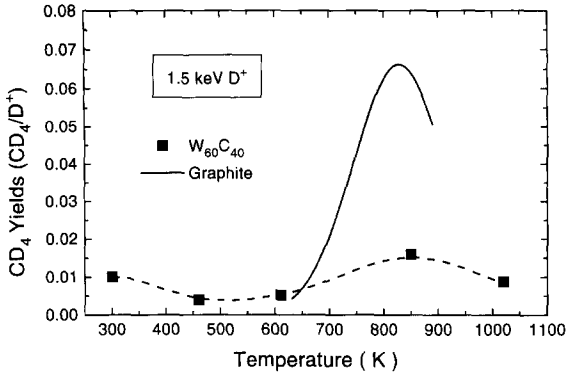

Fig. 2. Temperature dependence ofCD_4 release from $W_{60}C_{40}$ and graphite under 1.5 keV D^+ bombardment. The data of graphite are taken from Ref. [11] for comparison.

from $W_{60}C_{40}$ followed by a long decrease is also observed under bombardment with 3 and 0.8 keV D^+ at room temperature. The maximum value decreases with increasing incident energy. The threshold fluence, at which the CD_4 signal becomes visible, increases with the incident energy from 0.25×10^{17} D^+/cm^2 for 0.8 keV to 2×10^{17} D^+/cm^2 for 3 keV. These phenomena lead to the assumption that the methane molecules are formed and released from throughout the implantation range after diffusing to the surface. In contrast to graphite, where methane diffusion is too slow at room temperature to reach the surface [15], in $W_{60}C_{40}$ already at room temperature methane can diffuse within the ion range sufficiently fast.

Methane formation upon interaction of graphite with hydrogen ions has been investigated during the past two decades [11,16]. The maximum yield of methane was found during keV hydrogen implantation at 800–1000 K [17]. At room temperature the release of methane, about 0.035 CD_4/D^+, was observed only at very low ion energies below 100 eV [11,18]. After the implantation at room temperature in the keV range, the maximum of thermally desorbed methane was found at the temperature of 800–1000 K [19]. In this work significant release of methane from $W_{60}C_{40}$ is found, however, under keV D^+ bombardment at room temperature and the temperature dependence (Fig. 2) shows only a weak maximum round 850 K. In comparison with the total yield of WC for 1.5 keV D^+ of 0.01 measured by weight loss [18] the general level of the CD_4 yield of 0.005 shown in Fig. 2 suggests that all carbon atoms are eroded as methane molecules. Besides the methane release from $W_{60}C_{40}$, Fig. 2 also shows the temperature dependence of methane yields from pure graphite under 1.5 keV D^+ bombardment [11] for comparison. The maximum of methane release from $W_{60}C_{40}$, is 0.016 near 850 K corresponding to the temperature where the methane release from pure graphite also reaches a maximum, 0.065 CD_4/D^+. A similar suppression of chemical erosion with a weak temperature dependence was

also found in the interaction of TiC with keV hydrogen ions [13]. The dependence on ion energy at elevated temperature was found very similar to the physical sputtering of Ti indicating that the sputtering of the metal component was limiting the chemical erosion of carbon. The weak temperature dependence is expected, as the limiting process i.e. the physical sputtering of the metal component, does not depend on temperature. However, the peak in methane formation around 850 K indicates that at these temperatures carbon may diffuse from the bulk into the depleted layer leading to a temperature dependence similar to pure graphite. The increase towards room temperature was attributed in the case of TiC to adsorption of hydrocarbons from the residual gas and subsequent erosion as methane [13]. In the present case this can not be the origin of the slight increase, as for hot-rolled W sheet containing 3 at% carbon, IPS-W containing 10 at% carbon [6] or even $W_{85}C_{15}$ under deuterium bombardment both, at room temperature and elevated temperatures, the methane signal remains below the detection limit. It can not be ruled out, that the higher methane signal at room temperature for $W_{60}C_{40}$ may not represent a steady state erosion yield and may decrease to values as observed between 400 K and 600 K.

3.2. Deuterium retention and thermal desorption

The amount of deuterium retained in the target after implantation is calculated by integrating the difference between implanted and re-emitted deuterium fluxes over the implantation time until saturation. After 1.5 keV D^+ bombardment at room temperature we found that the amounts of trapped deuterium are 3.3×10^{17} at/cm^2 for $W_{60}C_{40}$ and 3.1×10^{17} at/cm^2 for $W_{85}C_{15}$. Both values are similar to the inventory of deuterium in graphite under the same bombardment condition [20]. For 3 keV D^+ bombardment at room temperature, the amount of retained deuterium in $W_{60}C_{40}$ is 4.5×10^{17} at/cm^2 which is about a factor of 1.4 higher than the value taken under 1.5 keV D^+ bombardment due to a larger implantation range and is also closed to the deuterium inventory in graphite [21]. The deuterium trapping in tungsten has been investigated under 1.5 keV D^+ bombardment by Alimov et al. [6]. He found that after the bombardment at room temperature the amounts of deuterium trapped in IPS-W (inert gas plasma sprayed tungsten coating) and hot-rolled-W (powder-metallurgy tungsten sheet) are much higher than that trapped in tungsten crystal, CVD-W (chemical vapor deposited tungsten coating) and VPS-W (vacuum plasma sprayed tungsten coating). He suggested that the deuterium inventory in tungsten is dominated by the material structure. García-Rosales proposed that the amount of trapped deuterium strongly depends on the porosity of tungsten samples [22]. This mechanism can explain their experimental results that the amount of deuterium trapped in IPS-W (with a porosity of 15–20%) is much higher than that in

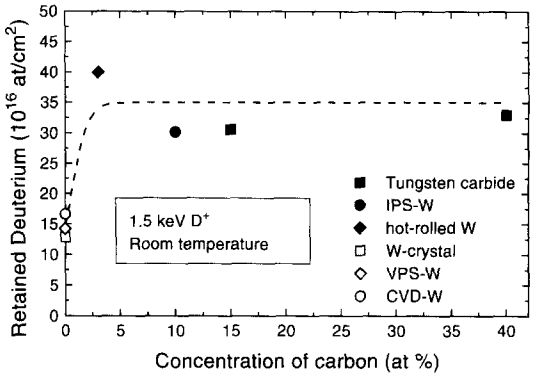

Fig. 3. Deuterium inventory in tungsten (open symbols), carbon-containing tungsten (solid circle and diamond) and tungsten carbide (solid square) after 1.5 keV D^+ implantation at room temperature. The data of tungsten are taken from Ref. [6].

VPS-W (with a porosity of 8–9%). However, it can not explain the high deuterium inventory in hot-rolled tungsten sample with a low porosity of $< 1\%$ and the low amount of trapped deuterium in VPS-W target with a high porosity of 8–9%. On the basis of the present results on tungsten carbide we suggest therefore that the carbon impurity is the key reason for the difference of D inventory in various tungsten materials. After the surface layer of about 100 nm was sputtered by 3 keV Ar ions, the XPS measurement reveals that the samples of W-crystal, CVD-W and VPS-W (all are produced in vacuum) are carbon-free materials and that the samples of IPS-W and hot-rolled W sheet respectively contain 10 at% and 3 at% of carbon impurity coming from their production process. Fig. 3 shows that the retained deuterium in tungsten carbide ($W_{60}C_{40}$, and $W_{85}C_{15}$) and in carbon-containing tungsten (IPS-W and hot-rolled-W) is more than double the value in carbon-free tungsten (W-crystal, CVD-W and VPS-W). Only a few percent of carbon impurities dramatically increases the deuterium inventory in tungsten. This phenomenon implies that a large amount of trapped deuterium are bound with carbon atoms located in an extended range up to μm in bulk. The trapped deuterium diffuses into bulk far beyond the ion range in tungsten probably due to the enhanced diffusion through pores or grain boundaries [6,22]. Based on the present result on tungsten carbide the much stronger binding with impurities, specially with carbon, should be considered.

The saturated amounts of deuterium due to the implantation at elevated temperatures are one order of magnitude lower than the value at room temperature and very closed to the deuterium inventory in pure tungsten at elevated temperatures. Fig. 4 shows the temperature effect on the deuterium trapping in tungsten carbide under 1.5 keV D^+ implantation up to saturation. For comparison, the trapping amount in graphite [20] and in tungsten [6] under the same bombardment condition are also shown in Fig. 4. For the

implantation at room temperature the retained deuterium in tungsten carbide and in carbon-containing tungsten are as high as the value in graphite and are more than double the value in carbon-free tungsten as indicated in Fig. 3. The dependence of the decrease on target temperature is quite different. For graphite the decrease is very slow until a steady value at high temperature. In contrast, we find that the trapped deuterium in tungsten carbide and in carbon-containing tungsten is sharply decreased at the temperatures between 300 and 550 K and then reaches the amount in carbon-free tungsten at higher temperatures. This result implies that the thermal desorption of deuterium from tungsten carbide will occur at temperatures much lower than that from graphite, just as the behaviour of tungsten reported in Refs. [6,22]. Fig. 5 confirms this point. The TDS spectrum from $W_{60}C_{40}$ shows three peaks during a heating period subsequent to an implantation with 1.5 keV D ions at room temperature. The first and second peaks are located at 410 K and 510 K, where the retained deuterium sharply decreases as shown in Fig. 4. The third peak is at the high temperature about 850 K just as the peak temperature for the thermal desorption from graphite. A broad TDS peak is found at the low temperature range for $W_{85}C_{15}$. Various spectral forms of thermal desorption from tungsten have been found with different peak temperatures [6,22], but the mechanism is not clear. The experimental results from Ref. [22] suggested that the peak temperature is dominated by the sample porosity. However, in the present experiment two CVD samples have similar mechanical properties such as porosity, grain size and surface roughness. The experimental conditions, including implantation energy, current, fluence and heating rate, were adjusted to be similar. The main difference is carbon concentrations of the material. As described above,

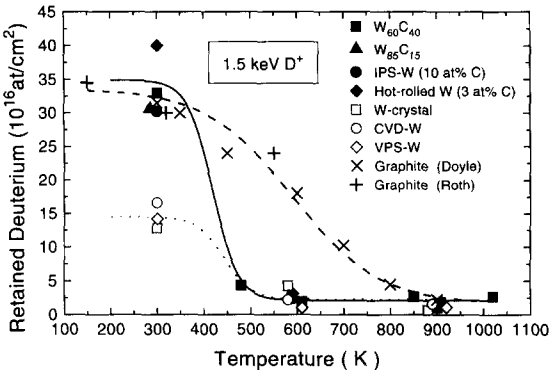

Fig. 4. Temperature dependence of deuterium inventory in tungsten carbide (solid square and triangle), carbon-containing tungsten (solid circle and diamond), carbon-free tungsten (open symbols) and graphite (cross) after 1.5 keV D^+ bombardment at different temperatures. The data of graphite are taken from Ref. [20] and the data of tungsten are taken from Ref. [6].

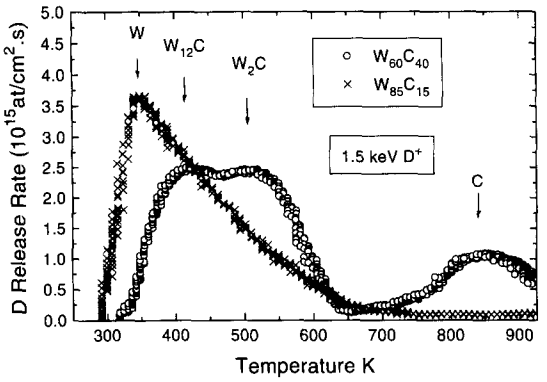

Fig. 5. Thermal desorption of deuterium from $W_{60}C_{40}$ and $W_{85}C_{15}$ subsequent to an implantation with 1.5 keV D^+ at room temperature. The different peaks correspond to the thermal release of deuterium bound to tungsten, tungsten carbide and carbon in the multi-phase samples.

the tungsten carbide coating consists of two carbide phases ($W_{12}C$ and W_2C) with 10–20 at% of free carbon atoms for $W_{60}C_{40}$ and with some free tungsten atoms for $W_{85}C_{15}$. The two TDS peaks located at low temperature range of 410 and 510 K may be corresponding to the thermal desorption of deuterium trapped in $W_{12}C$ and W_2C carbide with low binding energies and the peak at high temperature of 850 K corresponds to the desorption of deuterium strongly bound to carbon atoms. The broad TDS spectrum of $W_{85}C_{15}$ can be considered as an overlap of three peaks at temperatures of 350, 410 and 510 K. The first peak at 350 K is contributed by the desorbed deuterium bound to free tungsten atoms weakly. The thermal desorption spectrum, taken from $W_{60}C_{40}$ subsequent to an implantation with 3 keV D^+ at room temperature, is similar to the spectrum taken from the same target after 1.5 keV D^+ implantation as shown by open circles in Fig. 5, but the total amount of the trapped deuterium is higher by a factor of 20%. However, the thermal desorption spectra from tungsten made by different processes show a wide variety of forms in Ref. [6]. Both assumptions, from Ref. [22] and the present study, can only explain some of the results, but not all. Many factors, such as impurities, defects, structures and phases produced during target preparation or ion bombardment, lead to the complicated binding of deuterium with host, which results in the various TDS forms. A further study with identical target material is necessary for getting a good understanding.

The amount of trapped deuterium calculated by integrating TDS spectra over the heating time accounts for the results taken from re-emission measurements within 10–30%. This fact suggests that some of deuterium atoms bound to impurity with a higher binding energy or diffused to deep bulk are not desorbed from targets even at 1200 K, just as described by Alimov [6].

4. Conclusions

The amount of retained deuterium in tungsten carbide ($W_{60}C_{40}$ and $W_{85}C_{15}$) is similar to the value in pure graphite for the keV D^+ implantation at room temperature, which is more than double the value in pure tungsten. A few percent of carbon impurities in tungsten strongly increases the deuterium inventory up to the level as in tungsten carbide and in pure graphite. The deuterium inventory in tungsten carbide and in carbon-containing tungsten steeply decreases at the target temperatures between 300 to 550 K for the same implantation parameters as used at room temperature and reaches the value in pure tungsten at higher temperatures.

The thermal desorption of deuterium from tungsten and tungsten carbide occurs at temperatures much lower than for graphite and shows much more complicated spectral forms depending on many factors. In our case the different peak temperatures, 350, 410, 510 and 850 K are tentatively assigned to the release of deuterium from free tungsten, tungsten carbide ($W_{12}C$ and W_2C) and free carbon in the complex multi-phase samples.

The initial high methane release and the subsequent decrease with implantation fluence for tungsten carbide could be interpreted as the surface segregation of carbon induced by ion bombardment, which leads to a depletion layer throughout the ion range.

The low chemical erosion with a weak temperature dependence under keV D^+ bombardment for tungsten carbide suggests that the removal of the metal component by physical sputtering limits the chemical erosion of carbon. The weak maximum at a temperature around 850 K similar to pure graphite may be due to carbon diffusion from the bulk into the depleted layer.

References

[1] W. Eckstein and J. Roth, Nucl. Instrum. Methods B 53 (1991) 279.
[2] K. Krieger, V. Rohde, R. Schwörer, K. Asmussen, C. Garcia-Rosales, A. Hermann, R. Neu, J. Roth, A. Thoma, M. Weinlich and ASDEX Upgrade Team, these Proceedings, p. 734.
[3] H. Eleveld and A. van Veen, J. Nucl. Mater. 191–194 (1992) 433.
[4] J.W. Davis and A.A. Haasz, J. Nucl. Mater. 223 (1995) 312.
[5] A.A Pisarev, A.V. Varava and S.K. Zhdanov, J. Nucl. Mater. 220–222 (1995) 926.
[6] V.Kh. Alimov and B.M.U. Scherzer, J. Nucl. Mater., submitted.
[7] Yu.V. Lakhotkin and V.P. Kousmin, in: Proc. Int. Symp. on Advanced Technologies and Production of Organic and Inorganic Chemistry – 95, Moscow, April 25–28 (1995) section A, pp. 55–57.
[8] A. Krasovsky, R.K. Chuzhko, V.R. Tregulov and O.A. Balakhovky, Fluorine Process for Production of Tungsten (Nauka, Moscow, 1981) (in Russian).
[9] J. Ehrenberg, Max-Planck-Institut für Plasmaphysik, Report IPP 9/40 (1982).
[10] B.M.U. Scherzer, J. Ehrenberg and R. Behrisch, Radiat. Eff. 78 (1983) 417.
[11] J. Roth, E. Vietzke and A.A. Haasz, in: Atomic and plasma-material interaction data for fusion, Nucl. Fusion (Suppl.) 1 (1991) 63.
[12] P. Franzen, Max-Planck-Institut für Plasmaphysik, Report IPP 9/92 (1993).
[13] R. Yamada, K. Nakamura and M. Saidoh, J. Nucl. Mater. 111–112 (1982) 744.
[14] R. Schwörer et al., to be published.
[15] S. Chu, A.A. Haasz and P. Franzen, J. Nucl. Mater. 218 (1995) 319.
[16] J. Roth, in: Chemical Sputtering in Topics of Applied Physics, ed. R. Behrisch, Vol. 52 (Springer-Verlag, Berlin, 1983) p. 91.
[17] J. Roth and J. Bohdansky, Nucl. Instrum. Methods B 23 (1987) 549.
[18] W. Eckstein, C. García-Rosales, J. Roth and W. Ottenberger, Max-Planck-Institut für Plasmaphysik, Report IPP 9/82 (1993).
[19] R.A. Langley, R.S. Blewer and J. Roth, J. Nucl. Mater. 76–77 (1978) 313.
[20] B.L. Doyle, W.R. Wampler and D.K. Brice, J. Nucl. Mater. 103–104 (1981) 513.
[21] W. Möller, P. Børgesen and B.M.U. Scherzer, Nucl. Instrum. Methods B 19–20 (1987) 826.
[22] C. García-Rosales, P. Franzen, H. Plank, J. Roth and E. Gauthier, J. Nucl. Mater. 233–237 (1996) 803.